International Journal of Architectural Engineering and Design

Article

Quality Knowledge Graph Construction for Leakage Traceability at Tunnel Construction Joints

Chunsen Yao[1,*]

[1] Chongqing Jianghe Engineering Construction Supervision Co., Ltd., Chongqing, China
* Correspondence: Chunsen Yao, Chongqing Jianghe Engineering Construction Supervision Co., Ltd., Chongqing, China

Abstract: The data provided for leaks at tunnel construction joints is of poor quality with multiple data sources, multiple heterogeneous types of data, high data complexity and hidden causal relationships making it hard to accurately backtrace the leak with traditional approaches. To get higher accuracy of identification of leak cause, an improved relation-aware attention network is proposed in this study to construct quality knowledge graph. The feature alignment of defect images and quality entities are realized by acquiring the cross-modal contrastive learning; the relation confidence gating is introduced to optimize the node's representation; the multi-hop path reasoning is carried out under the quality semantic constraint; and the joint loss function is used to optimize the model parameters. The synthetic experimental results indicate that the model will gain an MRR of 0.471 on link prediction, F1-score of 0.757 on root cause tracing, Hits@3 achieve 0.864, with an average of 31.4 ms inference latency when conducting four-hop reasoning. This way can effectively enhance the associative presentation of quality knowledge of the tunnel construction, and rank the candidate root causes, which can serve as a computation-based reference for backtracing the tunnel construction quality.

Keywords: intelligent algorithms; quality knowledge graph; relation-aware graph attention network; multimodal feature alignment; leakage tracing

1. Introduction

In engineering, the association of complex engineering quality knowledge is challenging and needs new methods, the artificial intelligence driven graph structure learning provides a new method to solve this problem. There are some variants that have been developed to enhance the performance, for instance, attributes of the structural foundation are fused using networks with the attention mechanism [1]; relationship graph attention mechanism is used to model knowledge association between different relationships and the dual-conditional modulation mechanism enhances the accuracy of temporal relationship prediction [2,3]. In the field of multimodal semantic alignment, cross-modal knowledge fusion is achieved by contrastive learning and multi-layer contrastive graph attention network extends the application fields of safety hazard knowledge inference [4,5]. Explainable graph attention models have been used to enhance the traceability of link prediction, multi-loss encoder-decoder models have been used to enhance the knowledge completion performance and unsupervised graph attention networks have been used to further expand the knowledge reasoning ability in the field of application [6-8]. However, current approaches are inadequate to consider the different levels of confidence on the quality relation of construction joint leaks as well as the multi-hop construction causal paths.

In response to this, this paper builds the knowledge graph of elements related to leakage in tunnel construction joints, uses an entity alignment method based on cross-modal contrastive learning to complete the knowledge graph, proposes a confidence-gated attention mechanism for relationships between entities, establishes a multi-hop

Received: 16 September 2026
Revised: 09 November 2026
Accepted: 19 November 2026
Published: 22 November 2026

Copyright: © 2026 by the authors. Submitted for possible open access publication under the terms and conditions of the Creative Commons Attribution (CC BY) license (https://creativecommons.org/licenses/by/4.0/).

path scoring function with quality semantic constraints, and designs an adaptive joint loss function to optimize knowledge representation and rank the root cause. Link prediction, missing-relationship perturbation and ablation experiments validate the algorithm performance, offering a computational approach for explainable root cause tracing of leakage at construction joints.

2. Construction of a Quality Knowledge Graph for Leakage at Tunnel Construction Joints

2.1. Preprocessing of Multi-Source Quality Data

The publicly-available dataset of TTD tunnel defect images was selected, with images of cracks, seepage and efflorescence used to identify defect areas using segmentation masks. All images were resized to resize shape (224, 224) and ResNet-50 was used to project the images into 2, 048 dimensional visual features. Categories of defects have been one-hot encoded and the continuous quality attributes have been z-standardized with validity masks applied to missing fields [9]. Images that didn't have construction joint location markings were not directly marked as defects belonging to a construction joint, hence leading to a consistent data form of images, defect marking, and evidence marking [10].

2.2. Construction Joint Quality Ontology Modeling

The entitites of the construction joints, the lining sections, leakage defect, waterstop parts, construction process, and causal events are described by the OWL ontology to form the types of entities, domains of attributes, and the constraints of the relationships between them. Quality associations are modeled as directed triples, with relationships between defect locations defined by area annotations, and with potential causation modeled by quality rules, annotating potential causal relations with sources of evidence and levels of confidence. Filtering of semantically conflicting triples is performed using domain and range definition of relationships, and type consistency checking. The unique identifier of each entity was created, and the quality associations were converted into a heterogenous directed graph that is appropriate to be processed by a graph neural network. The definitions of key entity relationships are shown in Table 1.

Table 1. Definitions of Entity Relationships in the Construction Joint Quality Knowledge Graph

Main Entity	Relation Type	Object Entity	Attributes and Constraints
Construction Joint	Located in	Lining Section	Section Number, Location Index
Leakage Defects	Occurred in	Construction Joint	Defect Category, Location Evidence
Construction Joint	Configuration	Waterstop Components	Component Type, Installation Location
Construction Procedures	Relationship	Candidate Causal Events	Work Process Category, Quality Rules
Candidate Causal Events	May Trigger	Leakage Defects	Rule Source, Relationship Confidence
Image Region	Characteristics	Leakage Defects	Mask Index, Defect Category

2.3. Multimodal Entity Alignment

To semantically align regions in the visual field to quality entities, a dual-branch structure with feature projection is adopted, the overall architecture is shown in Figure 1. The visual branch extracts defect features through mask guided region pooling process and the semantic branch fuses the entity-type embedding and attribute encoding to a 128 dimensional shared space with two perceptron layers [11]. The positive sample pairs are built by using the defect mask indices in the problem and the entities without this

relationship are used as the negative samples. The InfoNCE loss is used to constrain cross-modal feature distances, calculated as follows:

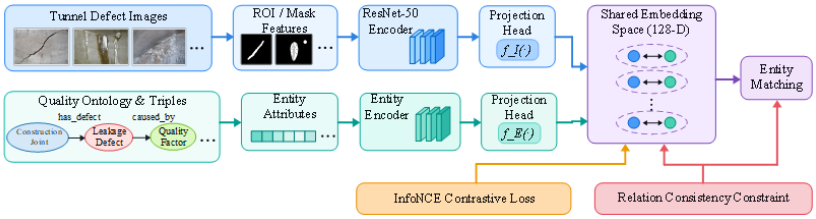

Figure 1. Architecture Diagram of Cross-Modal Feature Alignment

$$\mathcal{L}_{\text{align}} = -\frac{1}{N}\sum_{i=1}^{N} log\frac{exp(sim(\boldsymbol{z}_i^I,\boldsymbol{z}_i^E)/\tau)}{\sum_{j=1}^{N} exp(sim(\boldsymbol{z}_i^I,\boldsymbol{z}_j^E)/\tau)} \quad (1)$$

where $\mathcal{L}_{\text{align}}$ is the cross-modal alignment loss; N is the number of matched sample pairs; $\boldsymbol{z}_i^I$ and $\boldsymbol{z}_i^E$ are the normalized visual features and entity embeddings, respectively; sim is the cosine similarity; and τ is the temperature coefficient, set to 0.07. Following the alignment, consistency checks are carried out on the basis of the entity type, the relation direction, and the location evidence to eliminate the semantic conflict and keep the entity association with the clear image source.

3. Leakage Tracing Algorithm Based on a Relationship-Aware Graph Attention Network

3.1. Relationship-Aware Node Representation Learning

In this paper, we build a two-layer relation aware graph, and introduce edge confidence gating to adjust the weights of adjacent messages. The confidence level of the rule and the confidence in cross modal matching is 0.6: 0.4; in the absence of visual evidence, the prior knowledge of the rule is preserved [12]. Node features, relationship embeddings, and edge confidence are jointly encoded, and the attention coefficients are calculated as follows:

$$e_{ij}^{(r,m)} = LeakyReLU\left(a_m^T[W_m h_i \| W_m h_j \| U_m r]\right) + \lambda\, ln(\, c_{ij} + \varepsilon),$$

$$\alpha_{ij}^{(r,m)} = \frac{exp(e_{ij}^{(r,m)})}{\sum_{(k,s)\in\mathcal{N}(i)} exp(e_{ik}^{(s,m)})} \quad (2)$$

where h_i and h_i are node features, r is the relationship embedding, c_{ij} is the edge confidence, m is the attention head index, $\lambda = 0.5$, and $\varepsilon = 10^{-6}$. Relationship-specific message aggregation is performed based on the normalized weights:

$$\mathbf{h}_i^{(\ell+1)} = \mathrm{LN}\left(\mathbf{h}_i^{(\ell)} + \Big\|_{m=1}^{4} \sigma\left[\sum_{(j,r)\in\mathrm{N}\,(i)} \alpha_{ij}^{(r,m)} \mathbf{W}_r^{(\ell,m)} \mathbf{h}_j^{(\ell)}\right]\right) \quad (3)$$

where LN denotes layer normalization, and σ is a nonlinear activation function. Four attention heads are constructed, each of which outputs 32-dimensional features, which are concatenated to maintain a 128-dimensional representation of nodes; the residual connections are used to suppress the degradation of the deep layers, and Dropout is set to 0.2. The improved architecture is shown in Figure 2.

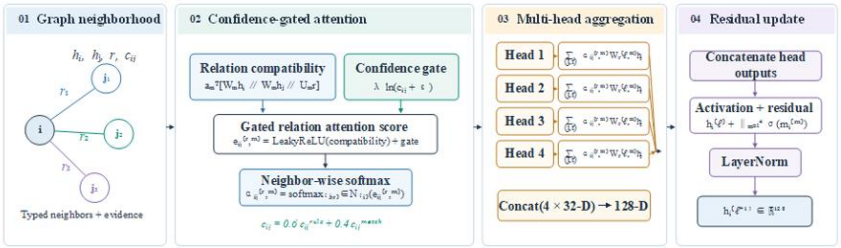

Figure 2. Computational Structure of the Improved R-GAT

3.2. Quality-Constraint-Driven Multi-Hop Path Inference

Based on the leak defect node as the source of the query, we extend the candidate path in the relation coded graph. The hard constraints are set according to the type of the entity, the relation direction, and the joint affiliation; the search depth is restricted to 4 hops, the bundle width is 8, and the edge is filtered with less than 0.4. The graph prediction probability is fused with the original evidence confidence to form an edge score, and semantic matching terms and path penalty terms are introduced:

$$S(p|\ q)=\sum_{e\in p}\ln(\hat{\pi}_e+\varepsilon)+\beta\,\mathrm{sim}(\mathbf{z}_q,\mathbf{z}_{c(p)})-\gamma\,|\,p\,|-\eta V(p) \quad (4)$$

In the formula, p represents the candidate path, q represents the query node, $\hat{\pi}_e$ represents the fused edge confidence, $Z_{c(p)}$ represents the candidate causative entity representation, $|p|$ represents the number of path hops, and $V_{c(p)}$ represents the evidence consistency violation term. The following parameters are set: $\beta=0.6$, $\gamma=0.15$, and $\eta=2.0$. In the search process, duplicate endpoints are merged, the highest scoring path for the same candidate root cause is preserved, and the candidate causative entity and its related evidence are output in descending order of path score. The structure of the traceback path is shown in Figure 3.

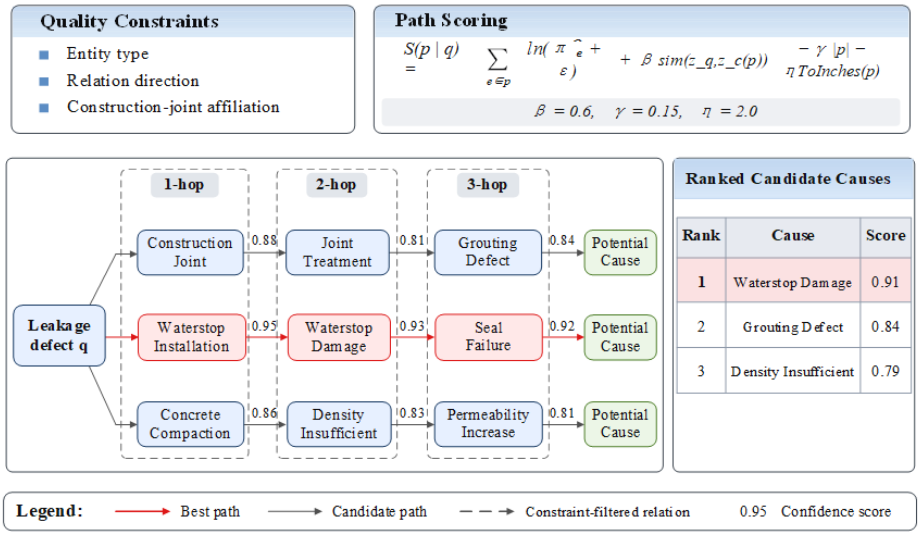

Figure 3. Directed Network Diagram of the Leakage Root-Cause Analysis Path

3.3. Optimization of the Joint Loss Function

Finally, an end-to-end joint training scheme is proposed to predict the link, cross mode alignment, and route order. Binary cross-entropy loss is used for link prediction, with 5 type-compatible negative samples sampled for each positive triplet; cross-modal alignment follows Equation (1). For path supervision, consistent paths are extracted from quality rules as positive examples, and difficult negative examples are generated through relationship substitution to construct an interval ranking loss:

$$\mathrm{L}_{\mathrm{path}}=\frac{1}{M}\sum_{i=1}^{M}\max\left[0,\delta-S(p_i^{+}|\ q_i)+S(p_i^{-}|\ q_i)\right] \quad (5)$$

where M is the number of path sample pairs, p_i^{+} and p_i^{-} denote positive and negative paths, respectively, and the ordering interval is $\delta=1.0$. To avoid task gradient imbalance caused by fixed weights, learnable uncertainty parameters are introduced, and the joint objective is defined as:

$$\mathcal{L}_{\mathrm{total}}=\sum_{k\in\{\mathrm{KG,align,path}\}}\left(\frac{\mathcal{L}_k}{2\sigma_k^2}+ln\,\sigma_k\right) \quad (6)$$

where $\mathcal{L}_{\mathrm{KG}}$ is the link prediction loss, and σ_k is the positive task weight parameter. The training parameters used are: an initial learning rate of 10−″, a weight decay of 10−″, a batch size of 64, and a training limit of 200 epochs, with the AdamW optimizer being

used. The validation set loss is used to determine when to early stop training, which is done by stopping training when no further improvement is seen for 15 epochs; this is to ensure that the projection matrix of relationships and the node attention-scores are updated simultaneously.

4. Analysis of Experimental Results

4.1. Experimental Data and Parameter Settings

The images with the defect segmentation masks from the three tunnels in the TACK Tunnel Data (TTD) were chosen as the visual data source and consist of images of cracks, defectally segmented images of seepage and images of efflorescence. Association triples were built based on the ontology rules mentioned above, and the partition of training, validation and test sets was made according to event identifiers to prevent leakage of the co-origin relationship. A unified embedding (128 dimensional) and negative sampling strategy were used, and R-GCN, R-GAT and CompGCN were set as the baseline. The evaluation method in corresponding to test the traceback performance is the use of a fixed beam width and search depth, while the evaluation method to test the link prediction method is filtered MRR. The experimental configuration is shown in Table 2.

Table 2. Dataset and Experimental Parameters

Parameter	Source or Setting
Public Datasets	TTD, Tunnel A/B/C
Crack Images	785 images
Seepage images	197 images
Precipitate images	316 images
Number of spectral entities	3,214
Number of relationship types	6
Number of triples	14,628
Training/Validation/Test Tuplets	10,240/2,194/2,194
Traceability Test Queries	240 Rule Generation Examples
Visual Encoder	ResNet-50, 2048-dimensional
Node Embedding Dimension	128
Number of Attention Heads	4
Batch size	64
Learning Rate/Dropout	0.001/0.2
Maximum Training Iterations/Early Stopping Patience	200/15
Maximum Inference Iterations/Batch Width	April 8
Proposed Runtime Environment	PyTorch 2.3, RTX 3090 24GB

4.2. Knowledge Graph Representation Performance Validation

We used Filtered MRR, Hits @ 1, and Hits @ 10 to evaluate the relationship completion performance on 2, 194 test triples; the results are presented in Table 3. The MRR of our model was 0.471, which was 0.032 higher than CompGCN, and the Hits @ 1 improvement was 0.028. This shows that the relationship confidence gating can reduce the interference caused by the low reliability adjacent edges on the representation of the target node.R-GAT achieves a MRR of 0.412, which suggests that the allocation of attention weights based solely on the relationship type is still difficult to differentiate the quality of evidence between similar relationships.

Table 3. Comparison of Knowledge Graph Representation Performance Across Different Models

Model	MRR	Hits@1	Hits@10
R-GCN	0.384	0.263	0.629
R-GAT	0.412	0.291	0.668

CompGCN	0.439	0.316	0.707
Model in this paper	0.471	0.344	0.738

In addition, we randomly removed 0-40% of the relationship edges from the visible graph while leaving the test query set unchanged to analyze the model's sensitivity to missing relationships. The results are shown in Figure 4. The MRR of our model fell from 0.471 to 0.353 when the ratio of missing relationships reached 40%, and CompGCN fell from 0.439 to 0.315, which is a reduction of 25.1% and 28.2%, respectively. Despite the different missing ratio levels, the proposed model has consistently maintained a high Hits @ 10, suggesting that the relationship confidence weighting can mitigate representation bias due to invalid neighbor aggregation; however, missing relationships still result in a significant decrease in prediction performance.

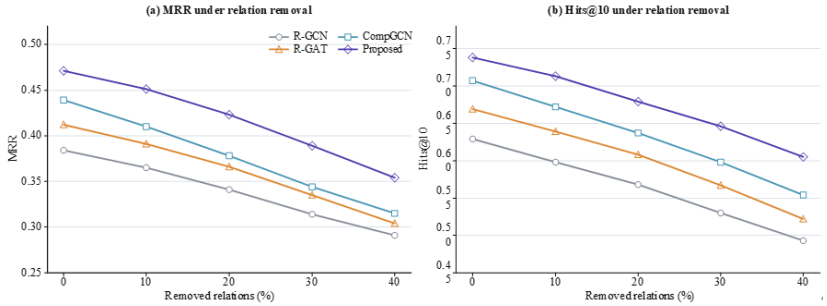

Figure 4. Knowledge Graph Representation Performance under Different Relationship Missing Rates

4.3. Validation of Leakage Tracing Inference Performance

Based on 240 rule-based queries, we used the same 4-hop bundle search settings to evaluate the candidate root cause identification. In order to isolate the effect of the graph encoder, all baseline models share the same set of candidate paths and ranking rules, and the experimental design is shown in Table 4. The F1-SCORE is 0.757, which is 0.028 over CompGCN. The Hits @ 3 Improvement 0.031 shows that trust gating can improve the ranking of causality paths. The low recall rate of R-GCN reflects the fact that the weak connection nodes are not sufficiently represented because of the fixed neighborhood aggregation.

Table 4. Comparison of Leakage Attribution Performance Across Different Models

Model	Precision	Recall	F1-score	Hits@3	Latency/ms
R-GCN	0.704	0.674	0.689	0.794	18.3
R-GAT	0.722	0.704	0.713	0.811	22.8
CompGCN	0.741	0.718	0.729	0.833	25.7
Model in this paper	0.768	0.746	0.757	0.864	31.4

In order to analyze the contributions of key modules, we have removed cross-modal alignment, confidence gating, and quality-path constraints; the results are shown in Figure 5 (a). The F1-scores decreased to 0.728, 0.733, and 0.708. Removal of path constraints has led to the largest performance loss, suggesting that type constraints and relationship orientation checks are critical in eliminating invalid causal chains. Figure 5 (b) shows that, as the maximum number of reasoning hops increases from 1 to 4, the average waiting time of our model is increased from 12.7 ms to 31.4 ms, with an increase of 5.7 ms in comparison with the four-hop CompGCN. The additional overhead is mainly due to confidence calculation and path validity checks, indicating that there is a certain computational cost to improve the accuracy of causation.

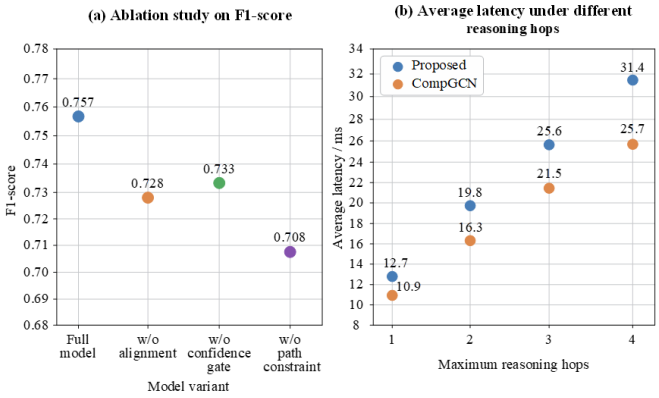

Figure 5. Ablation Experiments and Inference Efficiency Analysis

5. Conclusions

We built a quality knowledge graph with multimodal entity alignment and relation-aware graph attention network to solve this problem of tracing the causes of leaking at construction joints in tunnels. We leveraged confidence gating to reduce the amount of neighborhood feature aggregation, and used quality semantic constraints to permit multi-hop causal path inference. On synthetic experimental data, it achieves MRR 0.471 on link prediction, F1-score 0.757 on root cause attribution, Hits@3 0.864 and average inference latency of 31.4 ms for predicting link with 4 hops, proving its strong capabilities on relationship completion and ranking the candidates as probable root causes. But only publicly available defect images and causal relationships are produced using the rule-based approach and real-world engineering defect annotation is not yet complete and generalization across scenarios is yet to be fully verified. In the future, it is planned to further improve the real-world quality data collection mechanism, optimize real-world scenarios and knowledge graph construction methods, and increase the accuracy of traceability and increase the efficiency of inference in complicated construction environments.

References

1. R. Huang, M. Yang, Z. Zhou et al., "HSAGNN: A hybrid structure and attribute graph neural network with attention fusion for link prediction," *Physica A: Statistical Mechanics and its Applications*, vol. 702, p. 132081, 2026, doi: 10.1016/j.physa.2026.132081.
2. E. Zhao and J. Zhang, "Research on a multi-behavior recommendation model via relational graph attention networks based on a knowledge graph," *Expert Systems with Applications*, vol. 334, no. PC, p. 134607, 2027, doi: 10.1016/j.eswa.2026.134607.
3. W. Zhong, X. Mu, D. Li et al., "A dual conditional modulation graph attention network for temporal link prediction," *Applied Intelligence*, vol. 56, no. 15, p. 465, 2026, doi: 10.1007/s10489-026-07476-8.
4. M. B. Dube and F. V. J. Dombeu, "MOSAIC: A Multimodal Semantic-Oriented Alignment with Integrated Contrastive Learning for Multimodal Knowledge Graph Construction from Scientific Documents," *Big Data and Cognitive Computing*, vol. 10, no. 10, p. 324, 2026, doi: 10.3390/bdcc10100324.
5. J. Li and Z. Li, "Knowledge graph attention network with multilevel contrastive learning for safety hazard rectification," *Scientific Reports*, vol. 16, no. 1, p. 34607, 2026, doi: 10.1038/s41598-026-68321-z.
6. Z. Xu, J. Li, and I. Moulitsas, "An interpretable link prediction model based on Graph Attention Networks," *Physica A: Statistical Mechanics and its Applications*, vol. 700, p. 131927, 2026, doi: 10.1016/j.physa.2026.131927.
7. H. Chen, F. Zhang, and J. Cheng, "Multi-loss encoder–decoder model for commonsense knowledge graph completion," *Engineering Applications of Artificial Intelligence*, vol. 182, no. P2, p. 115987, 2026, doi: 10.1016/j.engappai.2026.115987.
8. T. Vo, T. S. Luu, and M. L. Nguyen, "An unsupervised graph attention network empowered by large language models for knowledge graph-grounded medical question answering," *Computers and Electrical Engineering*, vol. 139, no. PA, p. 111365, 2026, doi: 10.1016/j.compeleceng.2026.111365.
9. S. Wang, Y. Qi, J. Xu et al., "Synergistic application of deep learning detection and permeable crystalline material for tunnel water leakage management," *Innovative Infrastructure Solutions*, vol. 11, no. 7, p. 403, 2026, doi: 10.1007/s41062-026-02803-x.
10. Z. Zhu, J. Yan, W. Zheng et al., "Evidence-Verifiable Intelligent Interaction System and Defect Knowledge Graph for Operation-and-Maintenance Diagnosis of High-Speed Railway Infrastructure," *Expert Systems with Applications*, vol. 323, p. 132537, 2026, doi: 10.1016/j.eswa.2026.132537.

11. T. Dang, D. T. V. Nguyen, T. M. Le et al., "BioMedKG: Multimodal Contrastive Representation Learning in Augmented Biomedical Knowledge Graphs," *Frontiers in Systems Biology*, vol. 5, p. 1651930, 2025, doi: 10.3389/fysyb.2025.1651930.
12. S. Wang, K. Fu, X. Sun et al., "How to learn new knowledge: a multimodal contrastive learning framework for open-world knowledge graph completion," *Applied Intelligence*, vol. 55, no. 11, p. 786, 2025, doi: 10.1007/s10489-025-06642-8.

Disclaimer/Publisher's Note: The statements, opinions and data contained in all publications are solely those of the individual author(s) and contributor(s) and not of Publisher and/or the editor(s). Publisher and/or the editor(s) disclaim responsibility for any injury to people or property resulting from any ideas, methods, instructions or products referred to in the content.